Analytica Chimica Acta 853 (2015) 572–578

Contents lists available at ScienceDirect

Analytica Chimica Acta

journal homepage: www.elsevier.com/locate/aca

Analysis of organic acids and phenols of interest in the wine industry using Langmuir–Blodgett films based on functionalized nanoparticles

C. Medina-Plaza [a], C. García-Cabezón [b], C. García-Hernández [a], C. Bramorski [a], Y. Blanco-Val [b], F. Martín-Pedrosa [b], T. Kawai [c], J.A. de Saja [d], M.L. Rodríguez-Méndez [a,*]

[a] Department of Inorganic Chemistry, Engineers School, Universidad de Valladolid, Spain
[b] Department of Materials Science, Engineers School, Universidad de Valladolid, Spain
[c] Department of Industrial Chemistry, Tokyo University of Science, Japan
[d] Department of Condensed Matter Physics, Universidad de Valladolid, Spain

HIGHLIGHTS

- For the first time functionalized NPs immobilized in LB films have been used as voltammetric sensors.
- Films showed excellent electrocatalytic properties toward phenols and acids found in wines.
- Improved performance is due to combination of electrocatalytic NPs with the high surface/volume of LB films.
- The potential applications in the wine industry have been evidenced.

GRAPHICAL ABSTRACT

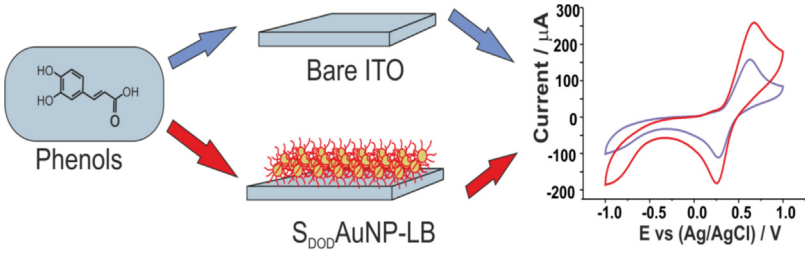

ARTICLE INFO

Article history:
Received 10 September 2014
Received in revised form 24 October 2014
Accepted 29 October 2014
Available online 1 November 2014

Keywords:
Langmuir–Blodgett
Gold nanoparticle
Phenolic compounds
Organic acids

ABSTRACT

A chemically modified electrode consisting of Langmuir–Blodgett (LB) films of *n*-dodecanethiol functionalized gold nanoparticles (S$_{DOD}$AuNP-LB), was investigated as a voltammetric sensor of organic and phenolic acids of interest in the wine industry. The nanostructured films demonstrated interfacial properties being able to detect the main organic acids present in grapes and wines (tartaric, malic, lactic and citric). Compared to a bare ITO electrode, the modified electrodes exhibited a shift of the reduction potential in the less positive direction and a marked enhancement in the current response. Moreover, the increased electrocatalytic properties made it possible to distinguish between the different dissociable protons of polyprotic acids. The S$_{DOD}$AuNP-LB sensor was also able to provide enhanced responses toward aqueous solutions of phenolic acids commonly found in wines (caffeic and gallic acids). The presence of nanoparticles increased drastically the sensitivity toward organic acids and phenolic compounds. Limits of detection as low as 10^{-6} mol L^{-1} were achieved. Efficient catalytic activity was also observed in mixtures of phenolic acid/tartaric in the range of pHs typically found in wines. In such mixtures, the electrode was able to provide simultaneous information about the acid and the phenol concentrations with a complete absence of interferences.

The excellent sensing properties shown by these sensors could be attributed to the electrocatalytic properties of the nanoparticles combined with the high surface to volume ratio and homogeneity provided by the LB technique used for the immobilization. Moreover, the LB technique also provided an accurate method to immobilize the gold nanoparticles giving rise to stable and reproducible

* Corresponding author at: Department of Inorganic Chemistry, Engineers School, Universidad de Valladolid Paseo del Cauce, 59, 4701 Valladolid, Spain. Tel.: +34 983 423540; fax: +34 983 423310.
E-mail address: mluz@eii.uva.es (M.L. Rodríguez-Méndez).

http://dx.doi.org/10.1016/j.aca.2014.10.046

sensors showing repeatability lower than 2% and reproducibility lower than 4% for all the compounds analyzed.

1. Introduction

The organoleptic and antioxidant properties of grapes and wines are closely related to their chemical composition. The organic acid content of grapes, musts and wines is of interest because its important influence on their sensory properties such as flavor, taste, color and aroma. Organic acids also affect the juice stability and are used as indicators of microbiological alterations in the beverage [1,2]. The principal organic acids found in grapes and therefore in wines, are tartaric and malic acids. Other acids such as citric acid are present in smaller amounts [3]. During the course of winemaking and in the finished wines other acids such as lactic acid can play significant roles.

Grapes and wines are also rich in phenolic compounds. Such compounds have attracted great interest due to their antioxidant activity and their important influence in the organoleptic properties [4,5]. In particular, phenolic acids, such as gallic and caffeic acids have been studied for their antioxidant capacity and for acting as venous dilators [6].

Various analytical methods have been reported for the determination of organic acids and phenolic compounds in wines and grapes including gas chromatography, HPLC, spectroscopic or electrochemical techniques [7–9]. Electrochemical measurements have certain advantages for the determination of antioxidants. For instance, the oxidation potentials measured by cyclic voltammetry (CV) have been used to compare the antioxidant strength of compounds such as phenolic acids, flavonoids, cinnamic acids, etc. being the glassy carbon electrode (GCE) the more frequently used electrode [10–14]. Chemically modified electrodes have also been successfully used as sensitive and selective tools for determination of many organic substances and some of them have been dedicated to the detection of organic acids and/or phenolic compounds [15–18]. Voltammetric electrodes have been successfully integrated in multisensor systems for the analysis of complex liquids [19,20].

Gold nanoparticles (AuNPs) have received great interest in the field of electrochemical sensors [21]. Their small size provides high surface to volume ratios that are the reason of their unique electronic and catalytic properties [22–26]. But in a number of applications, the benefits of using nanoparticles have not been fully exploited due to the lack of strategies for positioning the particles in ordered, homogeneous and reproducible solid-state devices. Recently, attempts have been made to immobilize NPs onto solid substrates using the Langmuir–Blodgett (LB) technique [27–30]. To obtain such ordered monolayers, nanoparticles must be capped to induce the amphiphilic character necessary for the LB technique [31].

Therefore, the aim of this work was to analyze the electrochemical and electrocatalytic properties of LB films of amphiphilic gold nanoparticles capped with *n*-dodecanethiol (S_{DOD}AuNP-LB) and to evaluate their capability to detect organic acids and antioxidant acids of interest in the wine industry. For this purpose, the main organic acids found in wines (tartaric, malic, lactic and citric acids) and two important phenolic acids including one diphenol (caffeic acid) and one triphenol (gallic acid) were analyzed by means of cyclic voltammetry. The electrocatalytic properties, the dynamic character and the detection limits were evaluated. The possible interferences caused by organic acids in the detection of phenols were also analyzed.

2. Experimental

2.1. Reagents and solutions

All experiments were carried out in deionized Milli-Q water (Millipore, Bedford, MA). Inorganic salts, organic acids (DL-malic acid, L(+)-tartaric acid and lactic acid), phenolic acids (caffeic and gallic acids), dodecanethiol, tetrachloroaurate tetrahydrate, tetraoctylammonium bromide and $NaBH_4$ were purchased from Sigma–Aldrich. Commercially available reagents and solvents were used without further purification.

10^{-3} mol L^{-1} stock solutions of organic acids and phenolic compounds were prepared by solving the corresponding compound in KCl (0.1 mol L^{-1}). Solutions with lower concentration were prepared from the stock solutions by dilution. The mixtures phenol/organic acid were prepared by mixing the corresponding volume of the 10^{-3} mol L^{-1} stock solutions in proportions 40:10; 25:25 and 10:40 to obtaining a final volume of 50 mL. The final concentrations of the mixtures were 8×10^{-4}:2×10^{-4}; 5×10^{-4}:5×10^{-4}; 2×10^{-4}:8×10^{-4} mol L^{-1}.

2.2. Apparatus

LB films were prepared in a USI-3-22 film balance (USI Co., Ltd.) equipped with a Wilhelmy plate to measure the surface pressure. TEM images were obtained using a Jeol JEM-1011 electron microscope operated at an accelerating voltage of 100 kV.

The electrochemistry was carried out in an EG&G PARC 273 potentiostat/galvanostat.

2.3. Preparation of nanoparticles

Dodecanethiol-functionalized Au nanoparticles (S_{DOD}AuNP) were prepared using the Brust's two-phase method [32]. A quantity 15.8 mL of a 24.3×10^{-3} mol L^{-1} aqueous solution of $HAuCl_4$ was added to a 2.9×10^{-3} mol L^{-1} phase transfer reagent, tetraoctylammonium bromide, dissolved in toluene (15 mL), and the mixture was stirred for 10 min. The toluene phase was subsequently collected and 1.5 mL of a 49×10^{-3} mol L^{-1} toluene solution of dodecanethiol (DOD) was added. The solution was stirred for 2 h. Then, 2 mL of a 2.11 mol L^{-1} aqueous solution of $NaBH_4$ was added. The reaction mixture was vigorously stirred at room temperature for 12 h, and the toluene phase was collected. Since the size distribution of the resulting S_{DOD}AuNP was quite broad, the dispersion was refluxed at 80 °C for 24 h to obtain monodisperse S_{DOD}AuNP. The resulting S_{DOD}AuNP were washed five times with acetone to remove the phase transfer reagent, excess DOD and reaction byproducts. The resulting particles have a narrow size distribution with an average diameter of 4.9 ± 0.5 nm.

2.4. Preparation of LB films

The toluene dispersion of S_{DOD}AuNP was spread onto the air/water interface to make the monolayer of Au NPs. The surface pressure-area (π-A) isotherm was measured at room temperature using a Wilhelmy balance. The monolayer of S_{DOD}AuNP was then transferred onto ITO substrates at a surface pressure of 10 mN m^{-1} to obtain LB films.

2.5. Electrochemical studies

The LB films were used as working electrodes of a conventional three electrode cell. The reference electrode was Ag|AgCl/KCl 3 M and the counter electrode was a platinum plate. Cyclic voltammetry was carried out at room temperature with a scan rate of 0.1 V s^{-1} in the potential range of −1.0 V and +1.0 V (vs. Ag/AgCl).

The repeatability of the voltammograms was evaluated from 5 repetitions on each sample. The reproducibility of data provided by the S_{DOD}AuNP was evaluated by comparing data provided by three sensors measuring identical samples in different days.

The dynamic character of the films was characterized by registering voltammograms at increasing scan rates from 0.01, 0.025, 0.050, 0.2, 0.5 to 1.0 V s^{-1}.

The calibration curves were constructed form solutions with concentrations ranging from 1×10^{-3} to 1×10^{-5} mol L^{-1}.

The limits of detection (LOD) were calculated following the 3SD/*m* criterion, where *m* is the slope of the calibration graph, and SD was estimated as the standard deviation ($n = 5$) of the voltammetric signals at the concentration level corresponding to the lowest concentration of the calibration plot [33].

3. Results

3.1. Structural characterization

Fig. 1 shows a TEM image of LB monolayer of S_{DOD}AuNP transferred on a TEM-copper grid at a surface pressure of 10 mN m^{-1}, which is the same transfer condition that we prepared S_{DOD}AuNP monolayer onto ITO substrates. S_{DOD}AuNP were in a relatively random array, but the single layer was densely covered with the substrate. The diameter of S_{DOD}AuNP was 4.9 ± 0.5 nm. The density of S_{DOD}AuNP was evaluated from the TEM image and found to be ~30 nm^2/particle.

3.2. Electrochemical response in simple electrolytes

As a first electrochemical characterization, cyclic voltammograms of bare ITO and of S_{DOD}AuNP-LB on ITO immersed in 0.1 mol L^{-1} solutions of different electrolytes (KCl, KBr, KNO_3, $KClO_4$ and $MgCl_2$) were registered. Fig. 2 compares the voltammograms obtained from a bare ITO and from a S_{DOD}AuNP-LB electrode in KCl and $MgCl_2$ solutions over a potential range from −1.0 to +1.0 V.

For the bare ITO electrode, no observable faradaic current appeared either on the forward or reverse scans regardless the electrolyte used. Whereas, the cyclic voltammogram for the S_{DOD}AuNP-LB modified electrode immersed in KCl (Fig. 2a) showed the typical response of gold nanoparticles with the oxidative peak at 0.7 V corresponding to gold oxide formation during the forward scan alongside the reduction peak at 0.17 V responsible for the reduction of gold oxide during the reverse scan [34,35]. The reduction of protons from water was promoted in the presence of S_{DOD}AuNP as indicated by the presence of a cathodic peak at ca. −0.75 V that was absent on neat ITO glass.

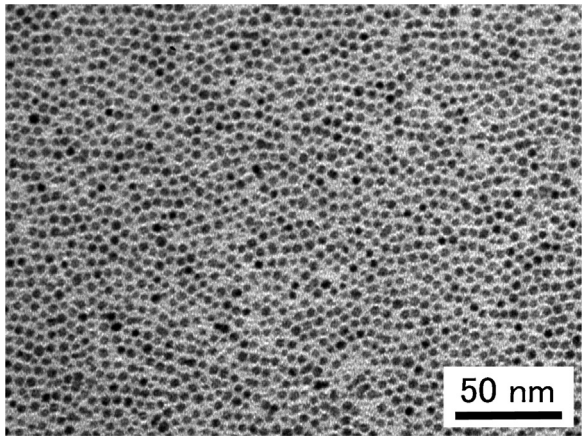

Fig. 1. TEM image of S_{DOD}AuNP LB monolayer transferred onto a TEM-copper grid.

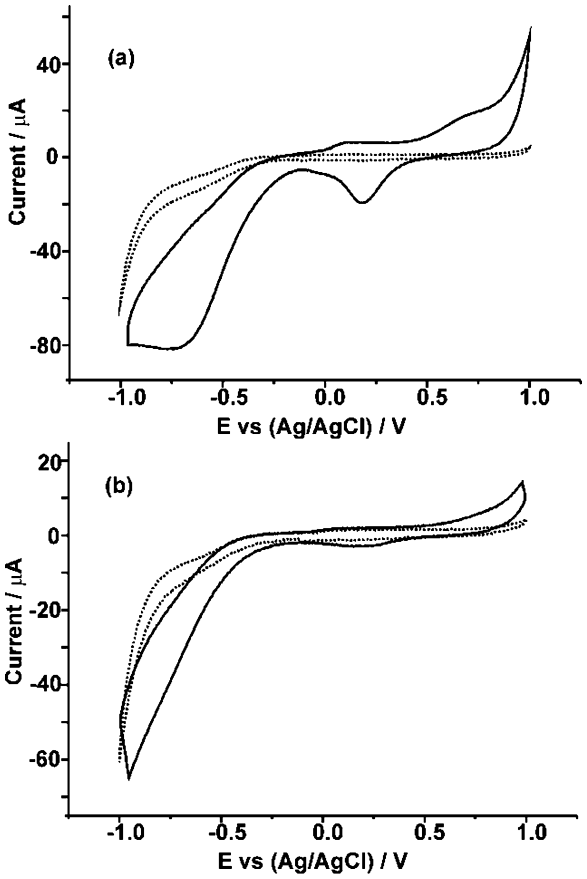

Fig. 2. Cyclic voltammograms of bare ITO (dotted line) and S_{DOD}AuNP-LB (solid line) sensors immersed in (a) 0.1 mol L^{-1} KCl and (b) 0.1 mol L^{-1} $MgCl_2$. Scan rate 0.1 V s^{-1}.

Voltammograms registered in the presence of other electrolytes containing potassium ion (KBr, KNO_3 or $KClO_4$) were quite similar. The peak positions did not change and only small modifications in the redox peak currents were observed. However, in the presence of divalent cations (such as Mg^{2+} from $MgCl_2$) the intensity of the redox peaks corresponding to gold oxidation/reduction decreased. Simultaneously, the peak corresponding to the reduction of protons from water was displaced to more negative potentials (Fig. 2b).

From these results, it can be concluded that cations instead of anions diffuse inside the films to maintain the electroneutrality during the scan. In addition, when the cation radius increased, the redox peak potential of the reduction of protons from water moved to more negative potentials decreasing the electrocatalytic activity of the S_{DOD}AuNP-LB sensor.

In all electrolytes analyzed, the intensity of the peaks increased linearly with the scan rate pointing to an electron transfer limited process (due to the electrochemical activity of the nanoparticles deposited at the surface of the electrode) with regression coefficients in the range of 0.990–0.995.

3.3. Electrocatalytic effect of S_{DOD}AuNP-LB toward organic acids

S_{DOD}AuNP-LB modified electrodes were used to analyze organic acids typically found in grapes and wines. The study included the

two main organic acids present in wines (tartaric and malic acids), one acid present in minor proportion (citric acid) – all of them coming from the oxidation of sugars –, along with lactic acid which is an example of acid generated by microbial activity. The electrocatalytic effect of S_{DOD}AuNP-LB electrodes was analyzed in 10^{-3} mol L^{-1} solutions of the corresponding organic acid by comparing the cyclic voltammograms observed at the bare ITO electrode and at the S_{DOD}AuNP-LB electrodes (Fig. 3).

None of the organic acids studied produced noticeable electrochemical responses when analyzed with a bare ITO electrode. However, the modified electrode catalyzed the reduction of the liberated protons and intense oxidation/reduction processes were observed at negative potentials.

The different electrochemical behaviors were related to the chemical nature of the acids analyzed. The voltammetric response of lactic acid (monoprotic acid, $pK_a = 3.90$; pH of a 10^{-3} mol L^{-1} sol. = 3.43) showed only one reduction peak at −0.85 V that corresponds to the reduction of the dissociated H^+ proton. In malic acid (diprotic acid; $pK_1 = 3.48$; $pK_2 = 5.10$; pH of a 10^{-3} mol L^{-1} sol. = 3.18), two well-separated electrochemical reduction peaks for each one of the dissociated protons were observed at about −0.85 V and −0.95 V. The corresponding oxidations occurred at −0.4 V and −0.5 V. The response of tartaric acid (diprotic acid; $pK_{a1} = 2.98$ and $pK_{a2} = 4.34$; pH of a 10^{-3} mol L^{-1} sol. = 2.93) also showed the reduction of the two protons (−0.85 V and −0.9 V). The oxidations were observed at −0.4 V and −0.5 V. It is important to notice that in tartaric acid, the redox peaks were not well resolved in both the forward and the reverse scans. It is also interesting to notice that the I_{pa}/I_{pc} ratio was much higher for tartaric acid than for malic acid. The fact that tartaric and malic acids showed different responses are of particular interest for the wine industry since tartaric and malic acids are the most prevalent acids present in wines. Moreover, malic acid shows a continuous decrease during ripening whereas tartaric acid remains almost unchanged. Therefore, different ratios can be obtained during ripening and the optimum harvest date can be established from their ratio.

The response of citric acid (triprotic acid; $pK_1 = 3.09$; $pK_2 = 4.75$ and $pK_{a3} = 6.41$; pH of a 10^{-3} mol L^{-1} sol. = 2.97) was similar to that of tartaric acid and two not well resolved cathodic peaks were observed. The similitude could be easily explained taking into account the weak acidity of the third acidic proton of the citric acid.

According to the enhancement in current responses, it is possible to conclude that S_{DOD}AuNP-LB electrodes show an intense electrocatalytic effect toward the reduction of protons, and that voltammetric responses are different for the main acids found in wines. In addition, the observation of distinct redox process associated with first and second dissociated protons is a remarkable result of our S_{DOD}AuNP-LB electrodes since bulk gold electrodes are not able to discriminate among acids or to provide distinct signals for different protons [36].

The influence of the potential scan rate on the peak height was also investigated between 0.01 and 1.0 V s^{-1}. The intensity of the cathodic peaks increased linearly with the square root of the scan rate and conformed to the Randles–Sevcik equation:

$$I = 2.69 \times 105 n^{3/2} A^{1/2} \nu^{1/2} c \quad (1)$$

where c represents concentration of the electroactive species, ν potential scan rate, A electrode surface, D diffusion coefficient of the analytes, and n number of electrons transferred in the redox process. In all cases, the correlation coefficient R^2 was higher than 0.9 pointing to a diffusion limited process (Table 1).

The logarithm of peak current changed linearly with the logarithm of scan rate (Table 1) with a slope value close to 0.5 for tartaric and lactic acids confirming ideal diffusion controlled

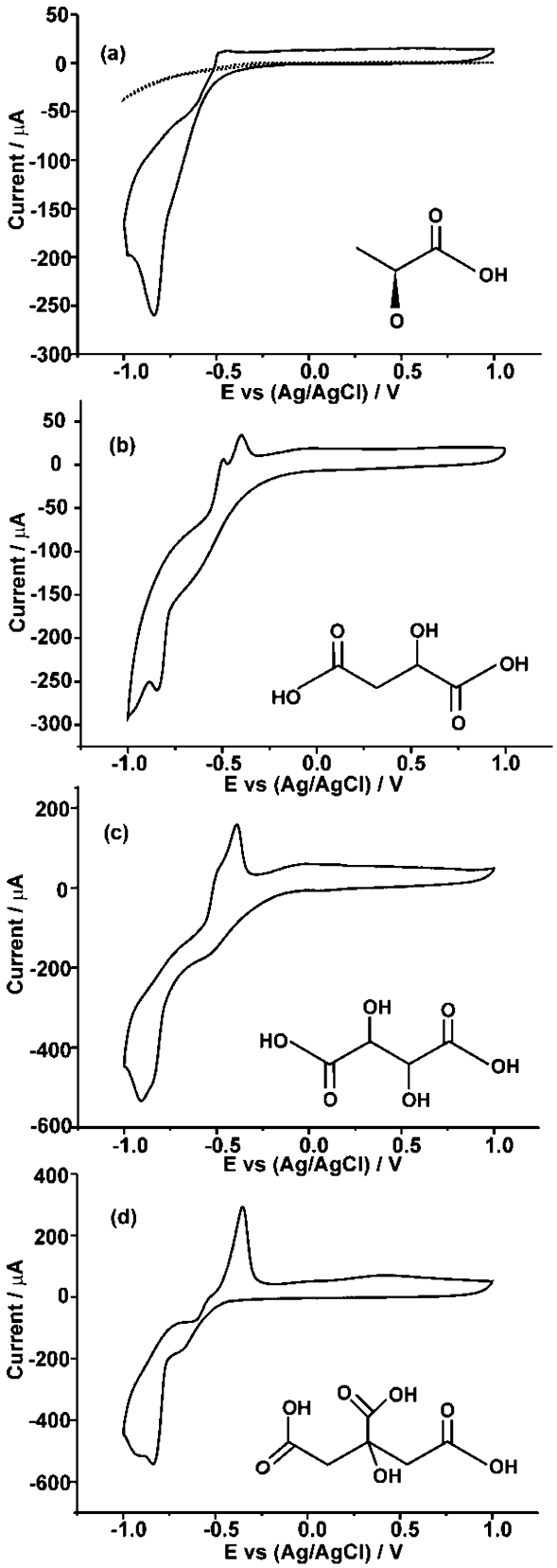

Fig. 3. CV of a bare ITO (dashed line) and S_{DOD}AuNP-LB (solid line) toward 10^{-3} mol L^{-1} of (a) lactic, (b) malic, (c) tartaric and (d) citric acids. Scan rate 0.1 V s^{-1}.

Table 1
Slope and regression coefficients obtained from the voltammograms registered at different scan rates for the organic acids. Intensities measured using the cathodic wave at −0.85 V.

Organic acid	Relationship with scan rate I_c (μA) vs. $\nu^{1/2}$ (mV s^{-1})$^{1/2}$		Relationship with scan rate log I_c (μA) vs. log ν (mV s^{-1})	
	Slope	R^2	Slope	R^2
Lactic	−24.14	0.990	0.48	0.990
Malic	−9.39	0.980	0.24	0.982
Tartaric	−47.15	0.992	0.45	0.991
Citric	−22.69	0.981	0.26	0.982

mechanism. In the case of citric and malic acids, the slopes were found to be lower than 0.5. A closer look to the graphs showed that the increase in the scan rate caused a shift of the cathodic peaks toward more negative potentials. At scan rates higher than 0.05 V s^{-1}, the peaks could not be observed for longer. The slopes recalculated for citric and malic acids using scan rates from 0.01 to 0.05 V s^{-1} were close to 0.4 pointing also to a diffusion controlled process.

In contrast, the anodic wave showed a tricky behavior. At low scan rates, a linear dependence with the square root of the scan rate was observed, but at scan rates higher than 0.5 V s^{-1} the voltammograms presented distorted shapes and decreased their intensity while a new broad peak at 0.5 V grew progressively. These facts could be explained assuming that adsorption/polymerization processes are involved in the oxidations, causing the mentioned distortion [37].

The effect of the concentration in the sensor response was studied by immersing the electrode in organic acid solutions with concentrations ranging from 1×10^{-5} to 1×10^{-3} mol L^{-1}. The influence of increasing concentrations is illustrated in Fig. 4 for citric acid. When representing the calibration curve for the cathodic peak (at −0.85 V), an increase in the intensity of the peaks with the concentration was observed. The limit of detection (LOD) calculated following the 3SD/m criterion, was 5.6×10^{-6} mol L^{-1} (Table 2). The anodic peak was only observed at concentrations higher than 10^{-4} mol L^{-1}. This observation could be explained taking into account the dissociation constants of the acids (pK_a) and the change of the pH caused by the concentration. The pH of a 10^{-3} mol L^{-1} citric acid solution ($CitH_3$) is 2.97 and the predominant species is $CitH_2^-$ whereas the pH of the 10^{-5} mol L^{-1} solution is 5.01 and the predominant species is $CitH^{2-}$, so, the anodic wave could only be observed when the dominant species was $CitH_2^-$. A similar behavior was observed in the rest of organic acids studied. For instance, tartaric acid can be present in wine and juice as tartaric acid (TH_2), bi-tartrate (TH^-) or tartrate (T^{2-}). The ratio of these depends mainly on the pH of the wine. The anodic

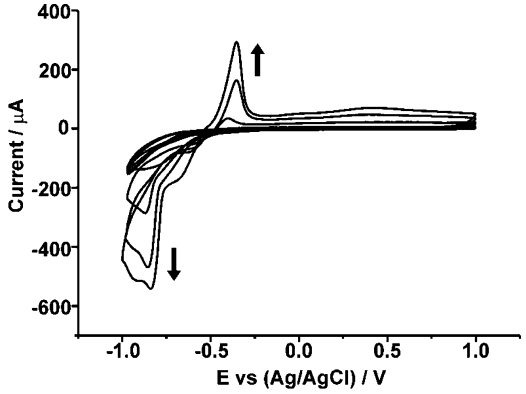

Fig. 4. CV of an LB film of S_{DOD}AuNP-LB immersed in increasing amounts of citric acid (10^{-5} to 10^{-3} mol L^{-1}).

Table 2
LOD, sensitivity and regression coefficient calculated from de cathodic peak at ca. −0.85 V for the four organic acids under study.

Organic acid	LOD (mol L^{-1})	Slope	R^2
Lactic	17.63×10^{-6}	−0.19	0.98
Malic	5.91×10^{-6}	−0.53	0.999
Tartaric	4.73×10^{-6}	−0.66	0.99
Citric	5.62×10^{-6}	−0.56	0.999

eave was only observed when the predominant species was bitartrate TH^- (maximum concentration of TH^- occurs at pH 3.7 and at pH 5.0, the predominant species is T^{2-}).

Due to the non-linear behavior of the anodic wave, in all organic acids analyzed the LODs were calculated by analyzing the intensity of the cathodic peaks at −0.85 V following the 3SD/m criterion. As observed in Table 2, they were in the range of 10^{-5} to 10^{-6} mol L^{-1}.

Taking into account that in the must obtained from grapes, tartaric acid is found in the range 3–7 g L^{-1},and malic acid in the range 1–3 g L^{-1} [38] the linear range and the LOD found here is adequate for the concentration usually found in such products.

3.4. Electrocatalytic effect of S_{DOD}AuNP-LB toward phenolic acids

Phenolic acids are also important ingredients of grapes and wines. Their interest relies in their antioxidant activity and in the key role they play in the organoleptic characteristics of wines. The electrochemical techniques are also appropriate to evaluate the antioxidant (or electrochemical) activity of the phenols. It has been established that the redox activity of these compounds can be measured using a glassy carbon electrode [10,15,39]. Depending on their chemical structure phenolic compounds can show low oxidation potentials (at ca. 0.5 V) or high oxidation potential (at ca. 0.8 V). In this work, the electrocatalytic effect of S_{DOD}AuNP-LB on the electrochemical response of two phenolic acids commonly found in wines, one with low oxidation potential (caffeic acid) and one with high oxidation potential (gallic acid) was analyzed (Fig. 5).

The electrochemical response of caffeic acid at a bare ITO was characterized by a redox pair with the anodic wave at 0.55 V and the cathodic at 0.25 V assigned to the oxidation/reduction of the diphenol to the *o*-quinone (Fig. 5a). The peak current of the electro-oxidation of caffeic acid at the S_{DOD}AuNP-LB sensor was clearly enhanced from 170 μA to 270 μA (an increase of the 75%) evidencing the catalytic effect of the modified electrode. The electrocatalytic effect was even more pronounced in gallic acid (a triphenol of high oxidation potential). As shown in Fig. 5b the gallic acid could not be oxidized nor reduced on a bare ITO glass at the potential range from −1.0 V to +1.0. However, at the modified electrode, an intense and irreversible peak appeared at 0.75 V. The enhancement in current response was a clear evidence of the catalytic effect of the S_{DOD}AuNP-LB modified electrode toward the oxidation of gallic acid.

The influence of the potential sweep speed on the peak height was studied in 10^{-3} mol L^{-1} solutions. The scan rate varied between 0.01 and 1.0 V s^{-1}. A linear increment in the redox peaks as a function of the square root of the scan rate was observed (with R^2 of 0.99) indicative of a diffusion-controlled electrode process. The relationship between the logarithm of peak current and the logarithm of scan rate was linear and the slopes were close to 0.5 (0.55 for caffeic acid, 0.42 for gallic acid). Thus, the diffusion controlled mechanism was further confirmed.

Voltammograms were registered using phenolic solutions with different concentrations. A linear relationship between the peak currents and caffeic acid concentration in the range between 1×10^{-3} mol L^{-1} and 1×10^{-5} mol L^{-1} was obtained. The LOD

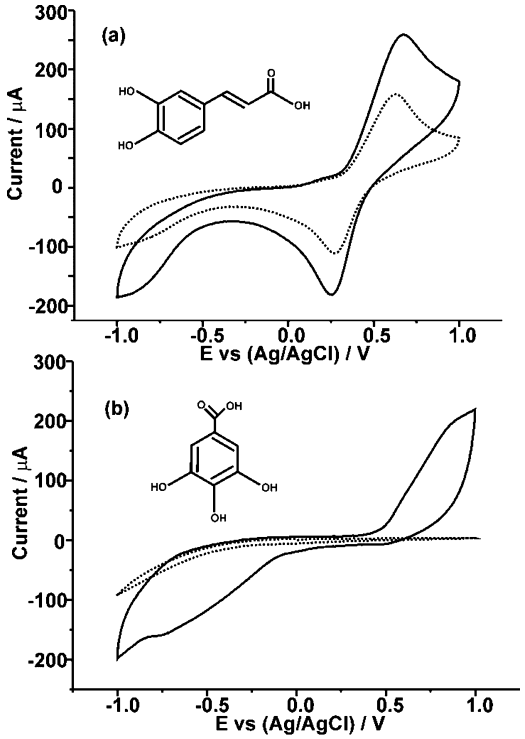

Fig. 5. Voltammetric response of a bare ITO electrode (dotted line) and a S_{DOD}AuNP-LB electrode (solid line) toward (a) caffeic acid and (b) gallic acid 10^{-4} mol L^{-1}.

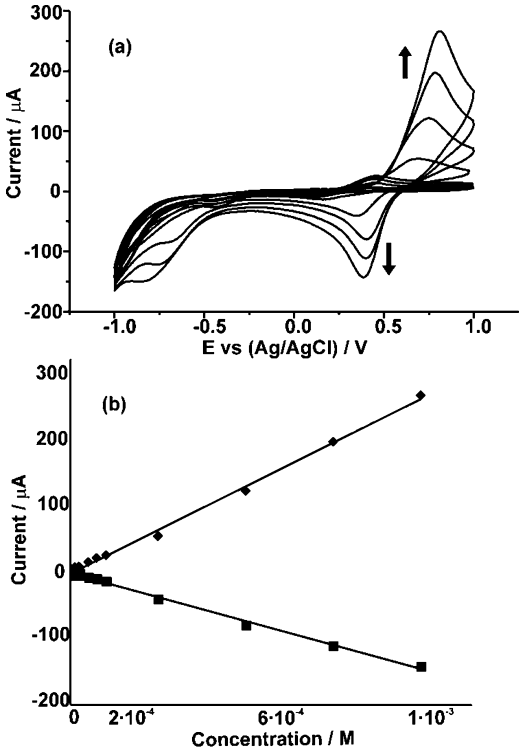

Fig. 6. (a) Cyclic voltammograms obtained for different caffeic acid concentrations from 10^{-5} to 10^{-3} mol L^{-1}; (b) calibration graph for the determination of caffeic acid.

calculated was 0.67×10^{-6} mol L^{-1} and 1.21×10^{-6} mol L^{-1} (for the anodic and cathodic peak, respectively). Simultaneously, the pH variation produced a progressive shift of the redox potential to higher values. This in good agreement with previously published studies that have proved that pH affects the redox potentials of the phenols [10]. CV plots recorded in gallic acid showed a similar behavior. A clear oxidation peak at ca. 0.75 V was observed that increased its intensity with the concentration (Fig. 6). The obtained calibration graph showed a linear dependence between peak height and gallic acid concentration acid (oxidation: $R^2 = 0.9968$/ reduction: $R^2 = 0.9969$). The LOD calculated according with the 3SD/m criterion was 0.51×10^{-6} mol L^{-1}.

This LOD obtained using the S_{DOD}AuNP-LB sensors was much lower than the values reported for glassy carbon electrodes (ca. 10^{-4} mol L^{-1}) [10] and similar to the LOD obtained using electrocatalytic films prepared from organic compounds [40]. It is also important to notice that the linear range was clearly enhanced with respect to that observed in glassy carbon electrodes, indicating that the contamination of the electrodes by the oxidation products is less important [41].

3.5. Response of S_{DOD}AuNP-LB toward mixtures of organic acids and phenols

In this section, experiments were made varying the acidity of the solution using mixtures of caffeic or gallic acids with tartaric acid (the majoritarian acid in wine and the main responsible of its acidity) in the range of pHs and concentrations found in wines. Experiments were carried out in caffeic:tartaric mixtures 40:10; 25:25 and 10:40 (corresponding to 8×10^{-4}:2×10^{-4}; 5×10^{-4}:5×10^{-4}; 2×10^{-4}:8×10^{-4} mol L^{-1}).

Fig. 7 shows the voltammetric responses of mixtures of caffeic and tartaric acid analyzed using the S_{DOD}AuNP-LB electrodes.

As expected, the intensity of both oxidation and reduction peaks, I_a and I_c, of the caffeic acid increased linearly with the concentration. At low concentrations of tartaric acid, the only peaks observed were produced by the oxidation/reduction of caffeic acid. Increasing amounts of tartaric acid decreased progressively the pH and the redox activity of the dissociated protons could be observed at negative potentials. Tartaric acid and caffeic acid did not show important interferences in the studied range, except a slight shift in the positions of caffeic acid due to the change in the pH caused by tartaric acid. The LOD obtained was similar to those obtained separately confirming the possibility of using the S_{DOD}AuNP-LB sensor for the simultaneous determination of acidity and caffeic acid in the range of concentrations usually found in wines. Similar results were obtained for gallic acid.

3.6. Electrode repeatability and reproducibility

To characterize the repeatability of the measures registered with the S_{DOD}AuNP-LB electrode, repetitive measurements were carried out in 10^{-3} mol L^{-1} solutions. For all the samples analyzed,

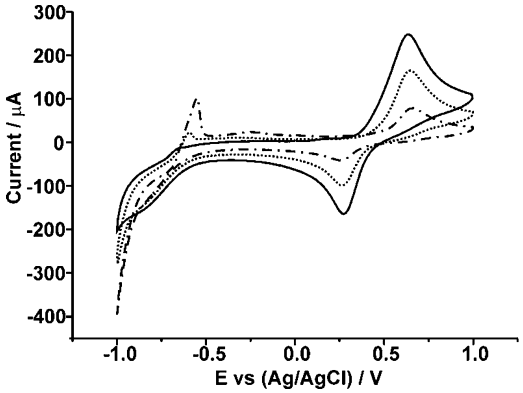

Fig. 7. CV registered using the S_{DOD}AuNP-LB electrode immersed in caffeic:tartaric mixtures. (solid) 40:10; (dotted) 25:25 and (slash-dotted) 10:40.

the results of 5 consecutive measurements showed a relative standard deviation (RSD) lower of 2%.

Also the reproducibility of the electrodes was examined by the determination of 10^{-3} mol L^{-1} caffeic acid using three electrodes prepared using the same method. RSD of anodic peak potential was found to be less than 4%, confirming the reproducibility of the method.

4. Conclusions

In this article, electrodes chemically modified with functionalized gold nanoparticles were achieved by the Langmuir–Blodgett technique. The modified S_{DOD}AuNP-LB electrodes demonstrated efficient interfacial properties being able to detect organic acids responsible of the acidity of grapes, musts and wines and phenolic acids with antioxidant properties. The LB technique applied to this amphiphilic nanoparticles produced sensors with high surface to volume ratios and efficient electrocatalytic behavior (increased peak currents) with limits of detection much lower than those obtained on ITO glass (in the range of 10^{-6} mol L^{-1}). In addition, the S_{DOD}AuNP-LB sensors were able to discriminate the predominant species indicated by the pK_a and the pH. Finally, it was possible to detect simultaneously organic acids and phenols. Interferences were not observed in the pH and concentration ranges found in wines and musts. According to these results, modified S_{DOD}AuNP-LB electrodes are good candidates to be a part of multisensor systems dedicated to the analysis of musts.

Acknowledgments

Financial support of the CICYT (Grant AGL2012-33535), Junta de Castilla y León (VA-032U13) and PIF-UVa is gratefully acknowledged.

References

[1] K. Ali, F. Maltese, Y.H. Choi, R. Verpoorte, Metabolic constituents of grapevine and grape-derived products, Phytochem. Rev. 9 (2010) 357.
[2] M. dos Santos Lima, I. de Souza Veras Silani, I.M. Toaldo, L.C. Corrêa, A. Camarão Telles Biasoto, G.E. Pereira, M.T. Bordignon-Luiz, J.L. Ninow, Phenolic compounds, organic acids and antioxidant activity of grape juices produced from new Brazilian varieties planted in the Northeast Region of Brazil, Food Chem. 161 (2014) 94.
[3] Y. Soyer, N. Koca, F. Karadeniz, Organic acid profile of Turkish white grapes and grape juices, J. Food Comp. Anal. 16 (2003) 629.
[4] D. Vauzour, A. Rodriguez-Mateos, G. Corona, M.J. Oruna-Concha, J.P.E. Spencer, Polyphenols and human health: prevention of disease and mechanisms of action, Nutrients 2 (2010) 1106.
[5] P.L. Teissedre, M. Jourdes, Tannins and anthocyanins of wine: phytochemistry and organoleptic properties, in: K.G. Ramawat, J.M. Mérillon (Eds.), Natural Products, Springer-Verlag, Berlin, Heidelberg, 2013 Chapter 72.
[6] I. Mudnic, D. Modun, V. Rastija, J. Vukovic, I. Brizic, V. Katalinic, B. Kozina, M. Medic-Saric, M. Boban, Antioxidative and vasodilatory effects of phenolic acids in wine, Food Chem. 119 (2010) 1205.
[7] Organisation Internationale de la Vigne et du Vin Recueil des methods internationals d'analyse des vins et des mouts, edition 2011, 8th Assemblée Générale, 21 June 2010, Paris (2011)
[8] J. Lee, Establishing a case for improved food phenolic analysis, Food Sci. Nutr. 2 (2014) 1.
[9] R. Prehn, J. Gonzalo-Ruiz, M. Cortina-Puig, Electrochemical detection of polyphenolic compounds in foods and beverages, Curr. Anal. Chem. 8 (2012) 472.
[10] P.A. Kilmartin, H.L. Zou, A.L. Waterhouse, A cyclic voltammetry method suitable to characterizing antioxidant properties of wine and wine phenolics, J. Agric. Food Chem. 49 (2001) 1957.
[11] R. Bortolomeazzi, N. Sebastianutto, R. Toniolo, A. Pizzariello, Comparative evaluation of the antioxidant capacity of smoke flavouring phenols by crocin bleaching inhibition DPPH radical scavenging and oxidation potential, Food Chem. 100 (2007) 1481.
[12] M. Abou Samra, V.S. Chedea, A. Economou, A. Calokerinos, P. Kefalas, Antioxidant/prooxidant properties of model phenolic compounds: part I. Studies on equimolar mixtures by chemiluminescence and cyclic voltammetry, Food Chem. 125 (2011) 622.
[13] K.E. Yakovleva, S.A. Kurzeev, E.V. Stepanova, T.V. Fedorova, B.A. Kuznetsov, O.V. Koroleva, Characterization of plant phenolic compounds by cyclic voltammetry, Appl. Biochem. Microbiol. 43 (2007) 661.
[14] J.F. Arteaga, M. Ruiz-Montoya, A. Palma, G. Alonso-Garrido, S. Pintado, J.M. Rodriguez-Mellado, Comparison of the simple cyclic voltammetry (CV) and DPPH assays for the determination of antioxidant capacity of active principles, Molecules 17 (2012) 5126.
[15] P.A. Kilmartin, H.L. Zou, A.L. Waterhouse, Correlation of wine phenolic composition versus cyclic voltammetry response, Am. J. Enol. Vitic. 53 (2002) 294.
[16] R.E. Schmitt, H.R. Molitor, T.S. Wu, Voltammetric method for the determination of lactic acid using a carbon paste electrode modified with cobalt phthalocyanine, Int. J. Electrochem. Sci. 7 (2012) 10835.
[17] C. Bianchini, A. Curulli, M. Pasquali, D. Zane, Determination of caffeic acid in wine using PEDOT film modified electrode, Food Chem. 156 (2014) 81.
[18] F. Matemadombo, C. Apetrei, T. Nyokong, M.L. Rodríguez-Méndez, J.A. de Saja, Comparison of carbon screen printed and disk electrodes in the detection of antioxidants using CoPc derivatives, Sens. Actuators B 166–167 (2012) 457.
[19] M. Gay-Martin, J.A. de Saja, R. Muñoz, M.L. Rodriguez-Mendez, Multisensor system based on bisphthalocyanine nanowires for the detection of antioxidants, Electrochim. Acta 68 (2012) 88.
[20] I.M. Apetrei, M.L. Rodríguez-Méndez, C. Apetrei, I. Nevares, M. del Alamo, J.A. de Saja, Monitoring of evolution during red wine aging in oak barrels and alternative method by means of an electronic panel test, Food Res. Int. 45 (2012) 244.
[21] M.C. Daniel, D. Astruc, Gold nanoparticles: assembly, supramolecular chemistry, quantum-size-related properties, and applications toward biology, catalysis, and nanotechnology, Chem. Rev. 104 (2004) 293.
[22] F.W. Campbell, R.G. Compton, The use of nanoparticles in electroanalysis: an updated review, Anal. Bioanal. Chem. 396 (2010) 241.
[23] J.M. Pingarron, P. Yañez-Señedo, A. Gonzalez-Cortes, Gold nanoparticle-based electrochemical biosensors, Electrochim. Acta 53 (2008) 5848.
[24] R.J. White, R. Luque, V.L. Budarin, J.H. Clark, D.J. Macquarrie, Supported metal nanoparticles on porous materials. Methods and applications, Chem. Soc. Rev. 38 (2009) 481.
[25] M.K. Fan, G.F.S. Andrade, A.G. Brolo, A review on the fabrication of substrates for surface enhanced Raman spectroscopy and their applications in analytical chemistry, Anal. Chim. Acta 693 (2011) 7.
[26] S.E. Baghbamidi, H. Beitollahi, S.Z. Mohammadi, S. Tajik, S. Soltani-Nejad, V. Soltani-Nejad, Nanostructure-based electrochemical sensor for the voltammetric determination of benserazide, uric acid, and folic acid, Chin. J. Catal. 34 (2013) 1869.
[27] L. Wang, X.H. Chen, X.L. Wang, X.P. Han, S.F. Liu, C.Z. Zhao, Electrochemical synthesis of gold nanostructure modified electrode and its development in electrochemical DNA biosensor, Biosens. Bioelectron. 30 (2011) 151.
[28] X.J. Huang, Y.K. Choi, Chemical sensors based on nanostructured materials, Sens. Actuators B 122 (2007) 659.
[29] T.A. Sanders, M.N. Sauced, J.A. Dahl, Langmuir isotherms of flexible, covalently crosslinked gold nanoparticle networks: increased collapse pressures of membrane-like structure, Mater. Lett. 120 (2014) 159.
[30] F.L. Supian, T.H. Richardson, A.V. Nabok, M. Deasy, M. Syahriman, Azmi nanoscale growth of CdS and PbS semiconductor within Calix [4] Arene Langmuir–Blodgett LB film for ion sensing application, Adv. Mat. 825 (2014) 520.
[31] S. Capone, M.G. Manera, A. Taurino, P. Siciliano, R. Rella, S. Luby, M. Benkovicova, P. Siffalovic, E. Majkova, Fe_3O_4/gamma-Fe_2O_3 nanoparticle multilayers deposited by the Langmuir–Blodgett technique for gas sensors application, Langmuir 30 (2014) 1190.
[32] M. Brust, J. Fink, D. Bethell, D.J. Schiffrin, C. Kiely, Synthesis and reactions of functionalised gold nanoparticles, J. Chem. Soc. Chem. Commun. (1995) 1655.
[33] Nomenclature. Symbols, Units and Their Usage in Spectrochemical Analysis-II Data Interpretation. Analytical Chemistry Division, IUPAC (1978)
[34] M.A. Alonso-Lomillo, C. Yardimci, O. Dominguez-Renedo, M.J. Arcos-Martinez, CYP450 2B4 covalently attached to carbon and gold screen printed electrodes by diazonium salt and thiols monolayers, Anal. Chim. Acta 633 (2009) 51.
[35] Y.Y. Fu, F.F. Liang, H.F. Tian, J.B. Hu, Nonenzymatic glucose sensor based on ITO electrode modified with gold nanoparticles by ion implantation, Electrochim. Acta 120 (2014) 314.
[36] J.D. Escobar, M. Alcaniz, R. Masot, A. Fuentes, R. Bataller, J. Soto, J.M. Barat, Quantification of organic acids using voltammetric tongues, Food Chem. 138 (2013) 814.
[37] J.F. Arteaga, M. Ruiz-Montoya, A. Palma, G. Alonso-Garrido, S. Pintado, J.M. Rodriguez-Mellado, Comparison of the simple cyclic voltammetry (CV) and DPPH assays for the determination of antioxidant capacity of active principles, Molecules 17 (2012) 5126.
[38] J.C. Cabanis, C. Flanzy, Oenologie, Technique & Documentation, Lavoisier, Paris, 1998.
[39] C. Apetrei, I. Apetrei, J.A. de Saja, M.L. Rodriguez-Méndez, Carbon paste electrodes made from different carbonaceous materials: application in the study of antioxidants, Sensors 11 (2011) 1328.
[40] E. Giuliani, R. Fernandes, L.C. Brazaca, M.L. Rodríguez-Méndez, J.A. de Saja, V. Zucolotto, Immobilization of lutetium bisphthalocyanine in nanostructured biomimetic sensors using the LbL technique for phenol detection, Biosens. Bioelectron. 26 (2011) 4715.
[41] M. Ferreira, H. Varela, R.M. Torresi, G. Tremiliosi-Filho, Electrode passivation caused by polymerization of different phenolic compounds, Electrochim. Acta 52 (2006) 434.